Study of the Time-Temperature-Dependent behaviour of PVB: application to laminated glass elements

F. Pelayo[1*], M.J. Lamela-Rey[1], , M. Muñiz Calvente[1], M. López-Aenlle[1], A. Álvarez-Vázquez[1] and A. Fernández-Canteli[1]

[1]Department of Construction and Manufacturing Engineering. University of Oviedo.

Campus de Viesques. 33203 Gijón. Spain

[*] fernandezpelayo@uniovi.es

Abstract.

The mechanical properties of viscoelastic materials are, in general, time and temperature dependent. For rheological simple viscoelastic materials, both variables can be related through the time-temperature-superposition (TTS) principle to construct the master curve of the material. The Willian-Landel-Ferry (WLF) equation is the most used model to relate curves corresponding to different temperatures in the glass transition zone. However, the fitting of the model to the experimental results leads to an undetermined system of equations. Therefore, a minimum experience in the fitting process is, in general, necessary in order to obtain accurate results.

In this work, the WLF-TTS method is applied to obtain the master curve of PVB (Polyvinyl-butyral). This material is widely used as viscoelastic core in laminated glass panels, which are commonly exposed to a wide range of temperatures.

Finally, the PVB mechanical characterization was used to simulate numerically the static and dynamic behaviour of laminated glass elements at different temperatures. The simulations were compared with experimental results being the errors less than a 2% for the static behaviour. For the dynamic behaviour, the natural frequencies were predicted with errors less than a 2.5%, whereas the discrepancies in the loss factors are less than 22%.

Keywords: Viscoelastic; material testing; mechanical properties; shift factors; laminated glass.

1. Introduction

The mechanical behaviour of viscoelastic materials is time and temperature dependent [1]. Therefore, when the viscoelastic mechanical properties of the material must be evaluated for practical applications, the temperature conditions and the duration of the loadings (time window) must be known.

This time and temperature dependence implies that a large number of assays should be carried out in order to cover all the material working conditions. However, in those so-called simply thermo-rheological materials [2], both variables (time and temperature) can be related through the Time–Temperature Superposition (TTS) principle [3, 4] so, a series of stretch time experiments at different temperatures can be shifted to a reference temperature in order to obtain a broad-band time master curve at the corresponding reference temperature (see Figure 1).

Although this principle is a valuable tool for obtaining the mechanical properties of viscoelastic materials that obey the TTS, an automatic method to shift all the curves does not exist. The shifting can be done manually, using overlapping guess algorithms or, i.e. a minimization interpolation process but, in any case, a good knowledge of the master curve construction process is required [5, 6]. A schematic description of the steps to develop a TTS fit is presented in Figure 1.

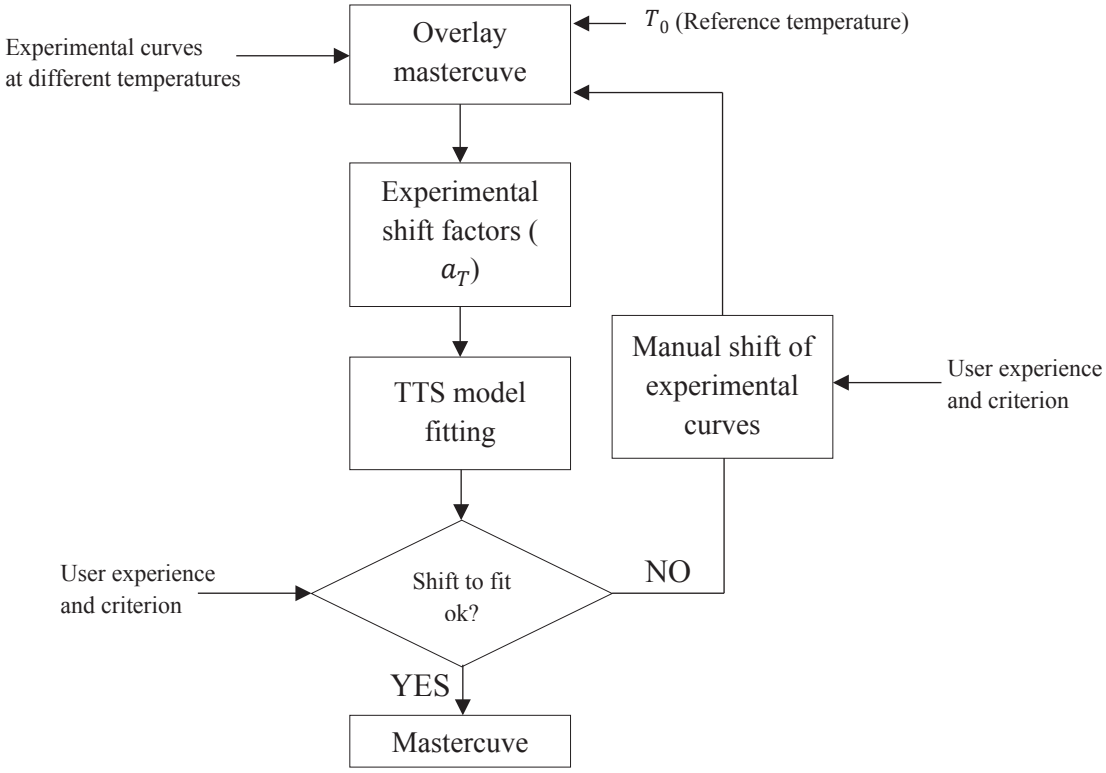

Figure 1. General steps of the time-temperature superposition method.

Several methods to determine the horizontal shift factor, a_T, that relates the temperature and time, have been proposed in the literature [7, 8]. However, within the glass transition zone, the WLF [9] model is widely used in the last 6 decades since a good agreement has been observed for a large number of materials.

Several authors use the WLF model to obtain the master curve at the reference temperature by simple overlapping without taking into account whether the fitting process or the constants of the WLF model

are acceptable. This procedure can imply that the master curve obtained at the reference temperature can only represent adequately the material behavior at a specific temperature range. Moreover, if the constants of the WLF model are wrong, the shifting of the master curve to other temperatures can also lead to large errors.

In this work, the WLF model is applied to determine the master curve of PVB, a material that is widely used as interlayer of simple (sandwich) or multilayered laminated glass elements [10]. Although the PVB interlayer thickness is much smaller than the glass layer thickness, the laminated glass behavior is highly dependent on the viscoelastic behavior of PVB. Therefore, viscoelasticity has to be taken into account in the design and calculations of laminated glass panels [11, 12].

The WLF model for PVB was obtained for both the relaxation modulus (time domain) as well as for the complex modulus (frequency domain) of the material using in both cases the corresponding experimental data. Different reference temperatures were considered to fit the model to the experimental results in order to validate the fitting process.

Furthermore, the master curve of the PVB was fitted to a Generalized Maxwell model using Prony series. The Prony coefficients of the material were also used to obtain the complex modulus of the material by analytical interconversions and compared with the experimental complex modulus of the PVB.

Finally, the PVB material model is applied to the analysis of laminated glass elements. Static and dynamic experiments were carried out in a laminated glass plate and a multi-layered laminated glass beam. The experimental results were compared with those obtained from a finite element model (FEM) using the viscoelastic mechanical properties obtained in this work.

2. Time-Temperature Superposition Principle: The WLF Equation

The main idea of the time-temperature superposition is to construct broadband time master curves (usually span several decades of time) from stretch time curves (2 or 3 decades) of the material obtained at different temperatures (see Figure 1). The principle can be applied indistinctly to the construction of any viscoelastic modulus, such as relaxation $E(t)$, creep $D(t)$ or complex $E^*(\omega)$. Hereafter, for the sake of simplicity the relaxation modulus $E(t)$ will be used but the methodology can be extended to the other viscoelastic functions in time or frequency domain, respectively.

To start the process of fitting a TTS model, an overlay master curve is necessary. The overlay master curve is initially obtained by overlapping the individual curves corresponding to the different temperatures tested (see Fig. 2). To produce the initial overlay master curve (see Figure 2), each individual curve at temperature T_i has to be horizontally time-shifted to the corresponding time interval in the overlay master curve at reference temperature T_0 (see Figure 2). That is:

$$E(t, T_0)_i = a_{T_i} E(t_i, T_i) \tag{1}$$

where $E(t,T_0)_i$ is the time-shifted curve, $E(t_i,T_i)$ is the original curve and a_{Ti} is the "time shift factor" (see Figure 2), hereafter, simply denoted as "shift factor".

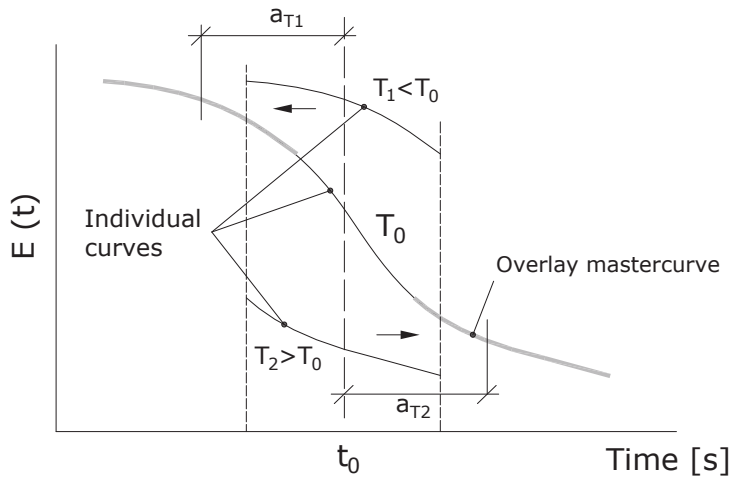

Figure 2: Schematic of the master curve creation process

In the glass transition zone, the WLF equation is widely used to obtain the horizontal shift factor, a_T, which relates the curves corresponding to two different temperatures, e.g. T and T_0 and which is given by [13]:

$$log a_T - \frac{B}{2.303}\left(\frac{1}{f} - \frac{1}{f_0}\right) + \log\left(\frac{T_0\,\rho_0}{T\,\rho}\right) \tag{2}$$

where f_0 is ratio of free to total volume of the molecules, B is an empirical constant and ρ_0 is the mass density. In practice, the last term of Eq. (2) can be neglected due to the slow temperature

variation of term ($T\ \rho$) [13]. If it is assumed the assumption that f increases linearly with temperature [13] by means of equation:

$$f = f_0 + \alpha_f(T - T_0) \tag{3}$$

where α_f is the thermal expansion of free volume relative to total volume. If Eq. (3) is substituted in Eq. (2), the classical expression of the WLF equation is derived [13]:

$$log a_T = -\frac{C_1^0(T - T_0)}{(C_2^o + T - T_0)} \tag{4}$$

where $C_1^0 = B/(2.303 f_0)$ and $C_2^0 = f_0/\alpha_f$ are empirical constants to be determinated in the WLF equation fitting process for the reference temperature T_0. The WLF equation cannot be solve directly since the two constants $C_1^0$and C_2^0 must be known. Therefore, additional techniques have to be used to fit the WLF model [13]. Alternative, the general values for constants $C_1^0$and C_2^0, proposed by Willian, Landel and Ferry, may be used [9, 13]. Once C_1^0 and C_2^0 are known for the initial reference temperature T_0, the WLF model can be used to evaluate the corresponding constants C_1^i and C_2^i at a different temperature, T_i, by means of the expressions:

$$C_1^i = \frac{C_1^0 C_2^0}{(C_2^0 + T_i - T_0)} \tag{5}$$

and

$$C_2^i = C_2^0 + T_i - T_0 \tag{6}$$

Therefore, the shift factors for a new master curve at reference temperature T_i can be obtained with Eq. (4) using the new constants C_1^i and C_2^i obtained with Eqs. (5) and (6), respectively. Although any temperature T_0 could be considered as reference in Eq. (4) during the fitting process, William, Landel

and Ferry [9] recommend the uses of the glass transition temperature (T_g) or better, an arbitrary temperature T_s, which can be approximated by [9]:

$$T_s \approx T_g + 50^oC \tag{7}$$

Once the master curve at temperature T_0 is created and the WLF constants are known, the complete family of mastercuves, for the range of validity of the WLF model, could be obtained (see Figure 3), so that, the time and temperature material viscoelastic modulus would be completely defined.

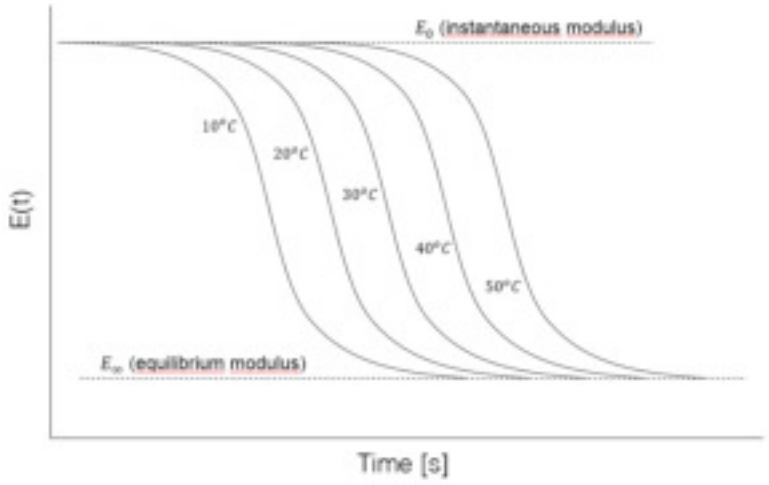

Figure 3. Example of relaxation modulus master curves at different temperatures.

3. Experimental Program

3.1 Experimental Equipment. A series of tensile relaxation test were carried out in a DMA RSA3 by T.A. Instruments. The DMA is equipped with a temperature-controlled chamber that conducts experiments over a wide range of temperatures, from -60^oC to 150^oC.

3.2 Material. The material used in the experiments was standard PVB (Polyvinyl butyral), an amorphous thermoplastic which shows a linear-viscoelastic behaviour [11, 14]. The specimens were 25 mm long and 5 mm wide and a thickness of 0.38 mm.

3.2 Experimental Testing. In order to obtain the relaxation master curve of the material, 15 tensile test were conducted at different temperatures from -15^oC to 50^oC. Additionally, 10 tests were conducted from 8 to 35 ^oC to obtain the complex modulus of the material. The experimental curves

are presented in Fig. 4 and 5 for the relaxation and complex moduli, respectively. In order to determine the range of applicability of the WLF model, a temperature sweep at 1 Hz was also carried out to estimate the glass transition zone of the material (see Fig. 6).

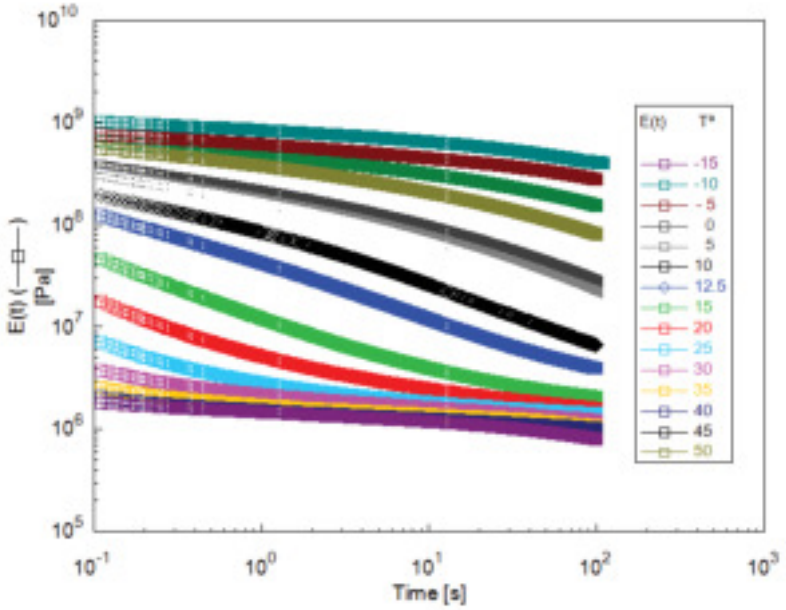

Figure 4: Relaxation curves at different temperatures for the PVB.

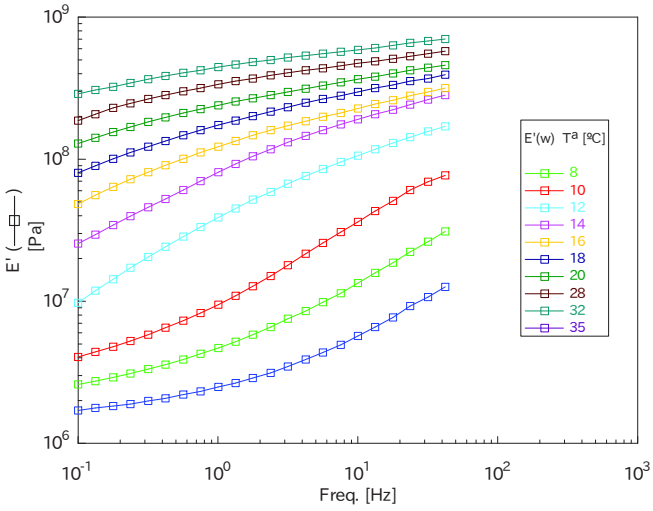

Figure 5: Storage modulus curves at different temperatures for the PVB.

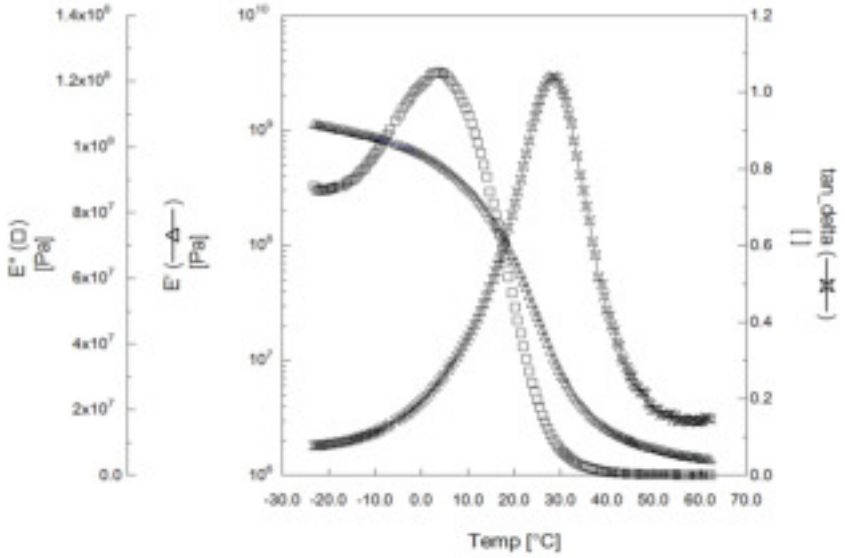

Figure 6: Temperature sweep at 1 Hz from -25^oC to 65^oC for the PVB.

4. Analysis of the Results

4.1 Glass Transition Temperature. Although there is not a unique procedure for determining the glass transition temperature [15], according to ASTM D3418-97 [16], T_g, can be inferred from the maximum peak of the loss modulus E'' obtained with temperature sweep analysis. In this case, T_g, is approximately at $+8^oC$.

4.2 Relaxation Master Curve of PVB. The initial overlay master curve of the material was obtained by overlapping the individual curves (see Figure 4), that is, each curve was horizontally shifted (only time-shifts were considered) to the reference one using a residual minimization algorithm based on cubic spline interpolation [17]. In Figure 7, it is shown the overlay master curve when 20^oC is used as reference temperature together with the experimental shift factors a_T^{exp}.

From Figure 7, it can be inferred that the material presents a thermorheological simple behavior [2], therefore, the technique of time-temperature superposition can be applied for obtaining the master curve of PVB. Once the overlay master curve is obtained the experimental shift factors, a_T^{exp}, for each curve can be estimated (see Fig. 7). It can be observed in Fig. 7 that a change in the tendency of the shift factors is observed when temperature falls from 10^oC. This fact agrees with the breakdown of the WLF TTS model at temperatures lower than the glass transition temperature of the material [9]. The phenomenon can be understood as a reduction of the free volume and mobility in the molecules,

so less variation of the material properties with temperature is expected and, consequently, a reduction in the corresponding shift factors should occur. This breakdown of the a_T^{exp} is also in agreement with the glass transition temperature $T_g = 8^oC$, obtained from Fig. 6, and must be taken into account to establish the range of validity of the WLF model. It must be emphasized that fitting all the temperature range (see Figure 7) with the WLF model will lead to erroneous constants C_1 and C_2 and, consequently, uncertainties and errors when the WLF model be used to shift the mastercuve of the material. In this way, 10^oC should be considered as the lower limit of applicability of the WLF model for PVB.

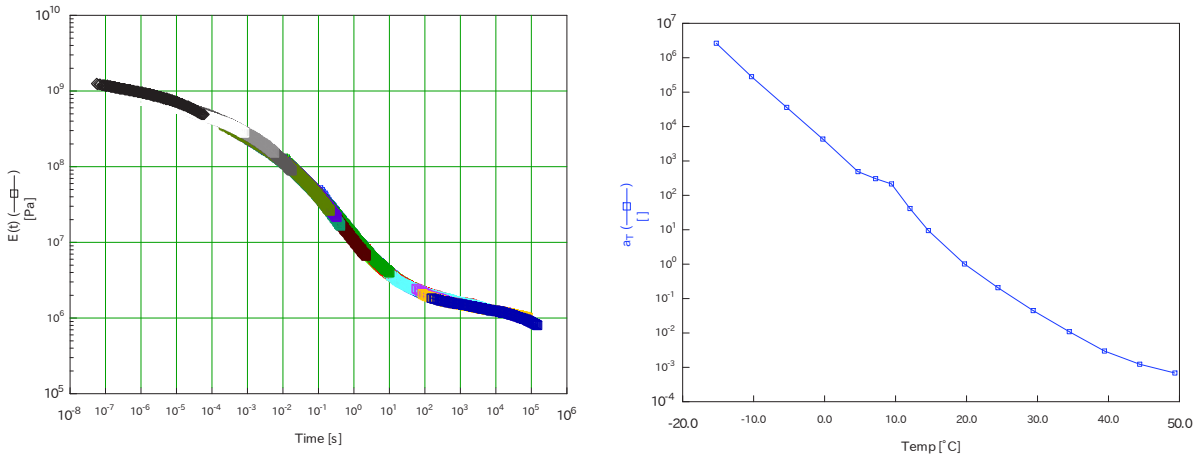

Figure 7: Overlay curve of PVB (left) and experimental a_T^{exp} (right) for a reference temperature of 20^oC

Although the WLF fitting process can be carried out taken T_g as the reference temperature, William, Landel and Ferry recommend to use in the fitting process a temperature T_s [9] (see Eq. (6)). This temperature T_s corresponds approximately to the end tail of the viscoelastic behaviour zone.

The WLF model (Eq. (4)) was fitted to the experimental results in the range from 10^oC to 50^oC using the shift factors a_T^{exp} shown in Fig. 7. These values were obtained considering $T_0 = T_s = 50^oC$ as reference temperature.

The parameters $C_1^s = 8.9932$ and $C_2^s = 104.76$ are close to the universal constants proposed by WLF: $C_1^{sWLF} = 8.86$ and $C_2^{sWLF} = 101.6$, the errors being about 1.5% and 3% for C_1 and C_2, respectively. If the WLF is fitted using T_g (in this case $T_g = 10^oC$) the following constants $C_1^g = 11.208$ and C_2^g

$= 41.818$ are obtained, that differ slightly from those proposed by WLF when T_s is used: $C_1^{gWLF} = 17.44$ and $C_2^{gWLF} = 51.6$. It has to be noticed that the universal constants proposed by WLF for T_g are obtained with an exact shift of 50^oC from T_s using Eqs. (5) and (6).

Whereas T_s and T_g are the reference temperatures recommended to fit the experimental data to the model (T_s being preferable [9]) , another temperature ion the range $T_g < T < T_s$ could be used in the fitting process, but the results obtained always present less accuracy than the other two cases (see Fig. 8).

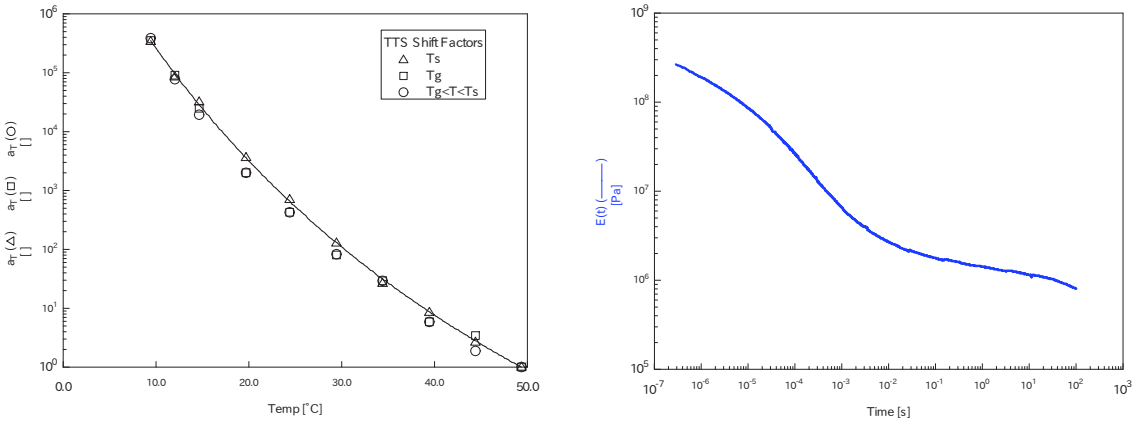

Figure 8. Comparison of the WLF model when T_s, T_g or a temperature within the range $T_g < T < T_s$ are used (left) and final master curve of the PVB for $T_s = 50^oC$ (right).

Once the WLF is fitted, the master curve of the PVB for reference temperature T_s can be constructed using Eq. (4) (see Fig. 8). The master curve at another temperature T_1, within the WLF temperature range ($T_g < T < T_s$), can be directly obtained shifting the master curve at 50^oC with the corresponding a_T estimated with Eq. (4) and constants C_1^s and C_2^s. The new constants C_1^1 and C_2^1 corresponding to temperature T_1 can be obtained with Eqs. (4) and (5), respectively. If temperatures lower than 10^oC must be taken into account, a new TTS model should be used to fit property the experimental shift factors below this temperature rather than use the a_T obtained with the WLF for the glass transition zone. In the case of PVB, the mechanical behaviour or laminated glass below the glass transition temperature can be assimilated to a monolithic glass with a thickness equal to the total thicknesses of the laminated glass elements [18, 19], Therefore, the TTS for PVB below 10^oC has less relevance from a practical point of view.

4.3 Complex modulus master curve of PVB

As a second step, the mastecurve for the dynamic complex modulus (frequency domain) of the PVB is obtained. The higher experimental temperature is for 35^o so in the WLF fitting process, this temperature was considered as reference. Although this temperature is below the recommended $T_s \approx T_g + 50^oC$, the lower storage values of the experimental curve at 35^oC (see Figure 5) are close to the minimum value of the material modulus, i.e. close to the low-frequency tail of the master curve and, therefore, can be considered adequate. The overlay curve for the complex moduli at 35^oC is presented in Figure 9 where the storage modulus (real part of the complex modulus) and the ratio $\tan\delta = E''/E'$, being E'' the loss modulus (imaginary part of the complex modulus) are shown.

The constants obtained for the WLF model at the reference temperature are: $C_1^{35} = 9.7240$ and $C_2^{35} = 97.0580$. Using Eqs. (5) and (6) these constants can be shifted to 50^oC, which corresponds with the value of T_s used for the WLF model in the relaxation master curve, being $C_1^{50} = 8.4128$ and $C_2^{50} = 112.0580$. If these values (C_1^{50} and C_2^{50}) are compared with those previously fitted for the relaxation modulus master curve ($C_1^s = 8.9932$ and $C_2^s = 104.76$), the errors are less than a 6.5% for both constants. If they are compared with the universal constants proposed for WLF at T_s, the errors are about 5% and 10% for C_1 and C_2, respectively, which are slightly higher than those obtained in the relaxation master curve. However, large errors are expected because the reference temperature $T_0 = 35^oC$ consider to fit the complex modulus is lower to the recommended T_s [9].

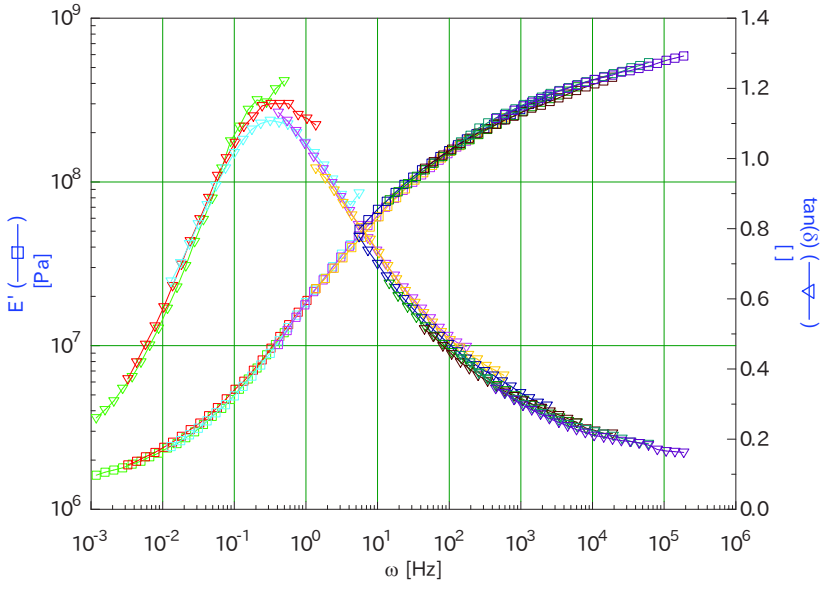

Figure 9. Overlay complex modulus curve for the PVB at 35^oC.

4.4. PVB viscoelastic model.

After fitting the WLF model to the experimental data, the mastercuve of both relaxation and complex modulus can be constructed. Although the master curves can be obtained for the complete time window of the overlay curves (see Figures 7 and 9), the WLF can be only used to shift both relaxation and complex moduli in the validity range i.e. 10^oC to $50^o\ C$.

A generalized Maxwell model [1, 2] was used to model the viscoelastic behaviour of the PVB. The model consist of several individual Maxwell models combined in parallel (see Figure 10).

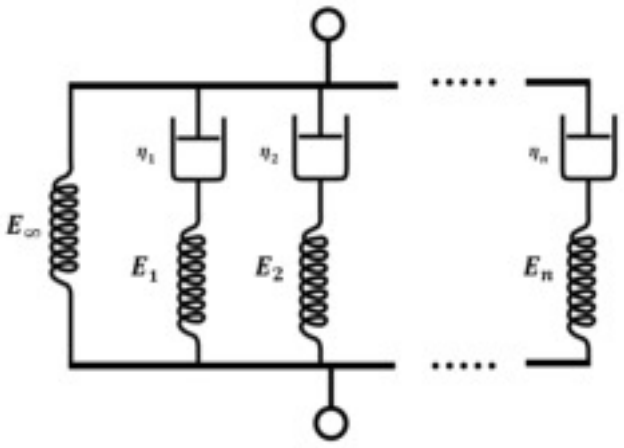

Figure 10. Generalized Maxwell model.

If the generalized Maxwell model is represented by a Prony's series [20], the relaxation Young modulus can be expressed as:

$$\mathrm{E(t)} = \mathrm{E_0}\left[1 - \sum_{\mathrm{i}=1}^{\mathrm{n_t}} \mathrm{e_i}\left(1 - \exp\left(-\frac{\mathrm{t}}{\tau_\mathrm{i}}\right)\right)\right] \tag{8}$$

where E_0 is the instantaneous modulus of the material, n_t is the number of Maxwell terms used in the model and (e_i, τ_i) are the Prony coefficients. The experimental master curve for a reference temperature $T = 20^oC$ and the viscoelastic fitted model using 13 terms in the Prony series (R-square 0.99943) are presented in Figure 9. The master curve at 20^oC was obtained by shifting the master curve at $T_s = 50^oC$ using the WLF model. The constants of the WLF calculated with Eqs. (5) and (6): being $C_{1R}^{20} = 12.6010$ and $C_{2R}^{20} = 74.7600$. The Prony coefficients for the viscoelastic model of the PVB are presented in Table 1.

Table 1. Prony series coefficients for PVB

e_i	τ_i [s]
2.342151953E-01	2.36600000000000E-07
2.137793134E-01	2.26430000000000E-06
1.745500419E-01	2.16668000000000E-05
1.195345045E-01	2.07327300000000E-04
1.362133454E-01	1.98389580000000E-03
6.840656310E-02	1.89837195000000E-02
4.143944180E-02	1.81653498300000E-01
7.251952800E-03	1.73822593210000E+00
2.825459600E-03	1.66329270788000E+01
2.712854000E-04	1.59158978189400E+02
4.293523000E-04	1.52297789909670E+03
9.804730000E-05	1.45732380763177E+04
5.274937000E-04	1.39449999999999E+05

Once the relaxation modulus of the material is known in terms of Prony coefficients, (e_i, τ_i), it can be used to obtain the components of the complex modulus by interconversion techniques, i.e. the storage modulus $E^{'}$ and the loss modulus $E^{''}$ [21, 22] are given by:

$$E^{'}(\omega) = E_{\infty} + \sum_{i=1}^{n} \frac{\tau_i^{2}\omega^{2}e_i}{\tau_i^{2}\omega^{2}+1} \tag{9}$$

$$E^{''}(\omega) = \sum_{i=1}^{n} \frac{\tau_i^{2}\omega^{2}e_i}{\tau_i^{2}\omega^{2}+1} \tag{10}$$

The complex modulus components of the PVB at $T = 20^{o}C$, obtained from the relaxation Prony coefficients using Eqs. (9) and (10), is presented in Figure 11 together with the experimental complex modulus master curve. The experimental complex modulus master curve has been shifted from 35^{o}C to $20^{o}C$ using the same WLF as that obtained by fitting the relaxation modulus. The WLF constants obtained using Eqs. (5) and (6) for 20^{o} were: $C_{1C}^{20} = 11.4885$ and $C_{2C}^{20} = 82.0580$, resulting in an error of 9% error when compared with those obtained from the WLF of the relaxation master curve.

From Figure 11, it is inferred than a good accuracy is also obtained using interconversion techniques (errors less than 10%), so that the WLF model proposed can be considered adequate to represent the

PVB mechanical behaviour in both time (relaxation modulus) and frequency (complex modulus) domains. On the other hand, similar constants C_1 and C_2 of the WLF model were obtained for both relaxation and complex moduli master curves, confirming that the WLF can be applied successfully to shift the master curve of the PVB at different temperatures. This fact is shown in Figure 9 where both predicted and experimental curves are shifted from 50^oC and 35^oC, respectively, to a reference temperature $T_0 = 20^oC$.

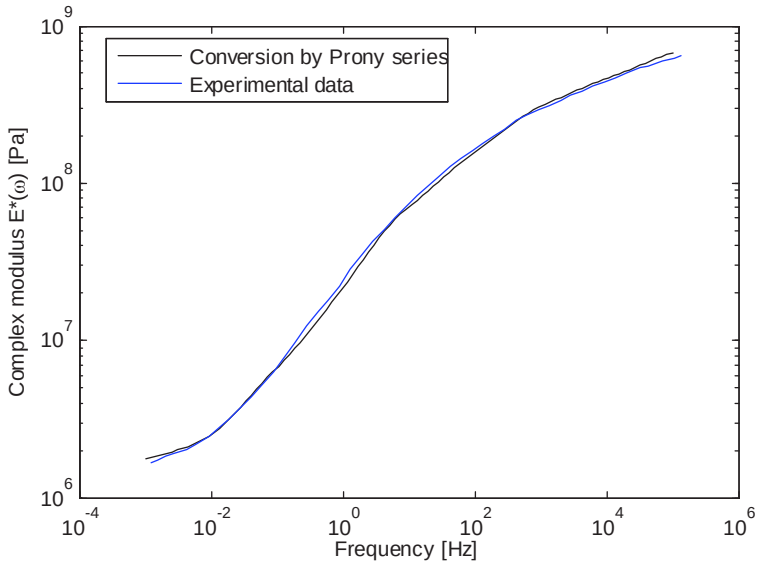

Figure 11. Complex modulus of the PVB obtained by interconversion from the relaxation Prony coefficients at 20^oC.

5. Practical application: laminated glass.

In order to validate the fitted WLF and viscoelastic Prony series models for the PVB, a static experimental test was carried out on a laminated glass plate and the modal parameters of a multilayered glass beam were estimated by operational modal analysis. The experimental results were compared with those provided by a finite element model where the mechanical behavior of the PVB was modelled using the parameters estimated in this paper.

5.1 Laminated glass plate under static loading.

A laminated glass plate pinned supported at the four corners with 4 wood balls (diameter of 50 mm) , dimensions $a =$ 1.4 m, $b = 1$ m and thicknesses $h_{glass} = 8$ mm for the glass layers and $h_{PVB} = 0.76$ mm for the PVB layer, respectively, was statically tested under an uniformly distributed

loading of 920 N/m^2. The experiment was conducted at 21.5^oC. The displacement of the central point of the plate was measured using a laser sensor (AR700-12) for approximately 26 hours with a NI-CDAQ system (NI9239).

In order to validate the mechanical properties of the PVB, a 3D finite element model was assembled in ABAQUS. 3D linear shell continuum elements (SC8R) were used for the glass layers [23] whereas the PVB layers were meshed with 3D linear hexahedral elements (C3D8R). This meshing technique has been demonstrated to be adequate to reproduce the laminated glass behavior with a relatively low computational time [24]. A detail of the mesh is shown in Figure 12. The elastic properties used for both glass and PVB are presented in Table 2. The mechanical behavior of the PVB interlayers was considered viscoelastic in terms of Prony series whose coefficients are shown (Table 1), whereas the WLF constants were $C_{1R}^{20} = 12.6010$ and $C_{2R}^{20} = 74.7600$.

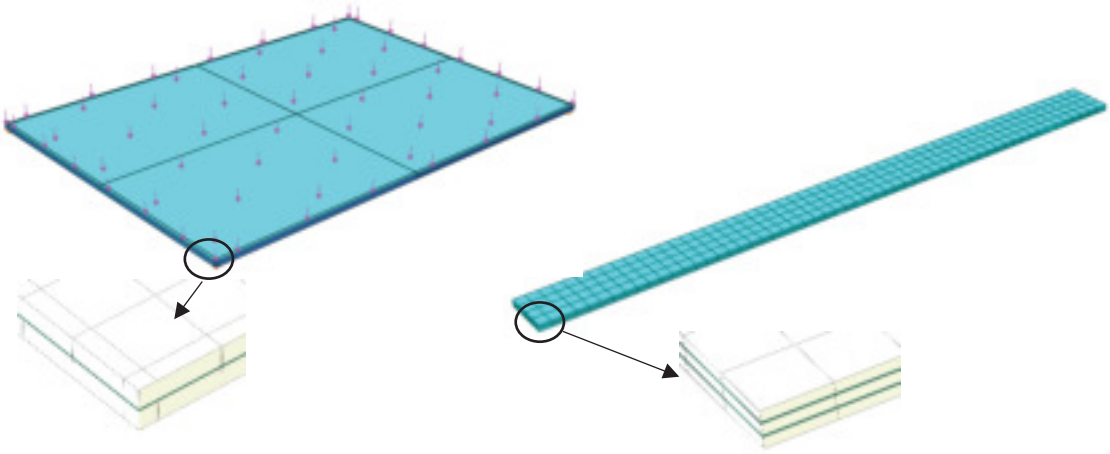

Figure 12. Finite element models for the laminated glass plate and beam.

Table 2. Mechanical properties of glass and PVB.

E_{glass} [GPa]	ν_{glass}	ρ_{glass} [kg/m^3]	$E_{0_{PVB}}$[GPa]	ν_{PVB}	ρ_{PVB} [kg/m^3]
72	0.22	2500	1.2403	0.40	1046

The experimental and numerical displacement at the central point of the plate are presented in Figure 13. It can be observed in the figure that a good correlation exists between the experimental and the simulated displacement the larger error being less than 1.75%.

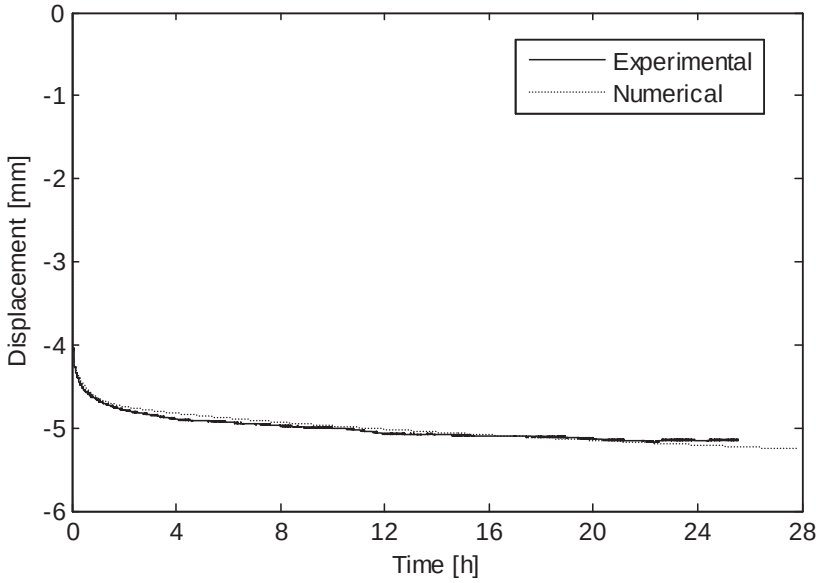

Figure 13. Displacement of central point of the laminated glass plate.

5.2 Multilayered laminated glass beam: dynamic behaviour

A multilayered laminated glass beam 1000 mm long and 100 mm wide thicknesses $h_{glass} = 4$ mm (3 layers) and $h_{PVB} = 0.38$ mm (2 layers) was used in the experiments. The beam was tested under free-free conditions using operational modal analysis [25]. Seven accelerometers (B&K: 100 mv/g) uniformly distributed along the beam were used to measure the responses and recorded with a NI-CDAQ system (NI9234). The beam was excited applying small hits along the beam random in time and space with an impact hammer and the responses were recorded for approximately 4 minutes using a sampling frequency of 1000 Hz. The modal tests were performed in a climate chamber at 20, 25 and 30 ºC, respectively. The modal parameters of the beam were estimate using the Frequency Domain Decomposition (EFDD) [25].

A 3D numerical model of the beam was also assembled in ABQUQUS meshing the glass layers with 3D linear shell continuum elements (SC8R) [24] whereas the PVB layers were meshed with 3D linear hexahedral elements (C3D8R). With respect to the the mechanical behavior, the same mechanical properties as those used in the plate were considered for the glass and the PVB interlayers (see Figure 12). In order to obtain the numerical modal parameters of the beam, the frequency response function (FRF) was obtained from a sweep sine analysis (linear frequency analysis) [24] subjecting the specimen to a uniform loading with a magnitude of 1 N for all the frequency range considered in the simulations. Then, the natural frequencies were estimated by the peak picking method [26, 27] whereas the damping ratios were obtained by the logarithmic decrement technique [26, 27].

The numerical natural frequencies and loss factors are presented in Table 3, together with those obtained experimentally. It is assumed that the damping ratios and the loss factors are related by $\eta \approx 2\zeta$ [28].

With respect to the natural frequencies, the error between the experimental and the numerical values was consistently less than 2.5%. On the other hand, large discrepancies were encountered in the loss factors, being the errors about 20% for the first mode at $T = 30^{o}C$. It has to be noticed that the uncertainty bounds of damping ratios (or loss factors) are usually much higher than those of the natural frequencies [29].

Table 3. Frequencies and damping ratios for the multilayered laminated glass beam at different temperatures.

T^a	Mode	Experimental		Numerical		Error	
		Freq. [Hz]	η [%]	Freq. [Hz]	η [%]	Freq. [%]	η [%]
20°C	1	36.14	1.18	36.58	1.26	1.19	7.16
	2	98.28	2.40	99.35	2.76	1.08	12.79
	3	188.94	3.24	191.18	3.72	1.17	12.78
	4	306.13	4.40	308.58	4.84	0.79	9.00
25°C	1	35.95	2.32	36.39	2.02	1.21	14.91
	2	96.56	4.22	97.87	4.30	1.35	2.30
	3	185.52	5.84	186.80	7.12	0.69	18.19
	4	297.53	8.74	300.61	8.82	1.03	1.10
30°C	1	35.40	5.66	35.95	4.44	1.54	21.55
	2	93.32	7.88	95.56	7.96	2.34	0.94
	3	175.72	10.82	180.02	11.46	2.39	5.69
	4	---	---	283.86	13.96	---	---

Conclusions

The WLF model and TTS have been used to obtain the relaxation master curve $E(t)$ of PVB. The most accurate results obtained when T_s is considered as reference temperature and the constants C_1 and C_2 obtained by fitting the experimental results are in good agreement with the general universal constants proposed by WLF.

The breakdown of the WLF model is in good agreement with the beginning of the Glass transition zone, so that the change in the slope of the experimental shift factors is a good indicator to establish the temperature limits of the WLF model. This breakdown may be used as a first estimation of the glass transition temperature (T_g) of the material being for PVB close to $8 - 10^{o}\ C$.

When using the WLF model, larger errors are obtained when a temperature between T_g and T_s (middle zone of the glass transition temperature) is used as the reference for the fitting process. This means that the master curve obtained at any reference temperature can represent adequately the material behaviour at this temperature. However significant discrepancies can appear when the master curve is shifted to another temperature using the WLF model fitted at a temperature $T_g < T < T_s$.

In this work, the WLF model was also applied to determine the complex modulus master curve $E^*(\omega)$ of the PVB. The WLF model for the complex modulus leads to approximately the same constants C_1 and C_2 (error less than a 6.5%) when compared with those obtained in the relaxation master curve $E(t)$. Although the different moduli of the material can be obtained from analytical interconversions, the fact that both relaxation and complex moduli give practically the same WLF model, confirms the validity of the model.

A generalized Maxwell model, expressed in terms of Prony series, has been fitted to the PVB relaxation master curve. The Prony series coefficients were then utilized to obtain the complex modulus of the PVB using Eqs. (9) and (10). Both experimental and analytical complex moduli master curve were shifted, respectively, to the same reference temperature ($T = 20^oC$) using the proposed WLF model. A good agreement was also obtained when the experimental and analytical complex master curve are compared (errors less than a 10%), i.e. the WLF model fitted in this paper can be considered adequate to represent the effect of temperature on the mechanical behaviour of PVB.

Finally, as a practical application of the PVB mechanical characterization, static and dynamic experiments at different temperatures were conducted in a laminated glass plate and a multilayered laminated glass beam, respectively. A finite element model of each laminated glass element was implemented in order to simulate the experimental results. The errors were less than a 1.75% for the static experiments, whereas in the dynamic experiments, the errors were less than a 2.5% for the natural frequencies being the uncertainties higher for the loss factors with a maximum error of 22%.

Acknowledgements

The authors gratefully acknowledge the financial support of the Asturian Regional Research through the Severo Ochoa Pre-doctoral Grants, as well as through the BIA2011-28959 and BIA2014-53774-R projects.

References

[1] Tschoegl, N.W.. The Phenomenological theory of linear viscoelastic behaviour. Springer-Verlag, Berlin (1989).

[2] Lakes, R., Viscoelastic solids. CRC Press, New York, (2009).

[3] Phan-Thien, N. On the time–temperature superposition principle of dilute polymer liquids, Journal of rheology. 23 (4), 451–456 (1979).

[4] Tobolsky, A.V., Properties and structure of polymers, Wiley, New York (1967).

[5] Dealy, J., Plazek D., Time-temperature superposition – A users guide. Rheology bulletin, 78(2), 16-31 (2009)

[6] Honerkamp, J., Weese, J., A note on estimating master curves, Rheologica Acta. 32(1), 57-64, (1993) doi: 10.1007/BF00396677.

[7] Sopade, P.A., Halley, P., Bhandari, B., D'arcy B., Doebler, C. and Caffin, N., Application of the Williams-Landel-Ferry model to the viscosity-temperature relationship of Australian honeys. Journal of food engineering, 56, 67-75 (2002)

[8] Povolo, F., Fontelos, M., General function with scaling properties and the time-temperature superposition. Il nuevo cimento. 13(12), 1513-1525 (1991)

[9] Williams, M.L., Landel, R.F., Ferry, J., The temperature dependence of relaxation mechanisms in amorphous polymers and other glass-forming liquids. Journal of the American chemical society, 77, 8701 (1955).

[10] Haldimann, M., Luible, A., Overend, M. Structural use of glass. Structural engineering documents (10). IABSE, (2008).

[11] Koutsawa, Y., Daya, E.M., Static and free vibration analysis of laminated glass beam on viscoelastic supports, International journal of solids and structures, 44, pp. 8735-8750 (2007).

[12] Galuppi, L., Royer-Carfagni, G.F., Laminated beams with viscoelastic interlayer, Journal of solids and structures, 49(18), 2637-2645 (2012).

[13] Ferry, J.D. Viscoelastic properties of polymers. John Wiley & Sons, New York (1980).

[14] Galuppi, L., Royer-Carfagni.. Localized contacts, stress concentrations and transient states in bent-lamination with viscoelastic adhesion. An analytical study. International journal of mechanics sciences. 103, 275-287 (2015).

[15] Rongzhi Li,. Time-temperature superposition method for glass transition temperature of plastic materials. Materials science and engineering. 278(1-2), 36-45 (1999).

[16] ASTM D3418-15 Standard test method for transition temperatures and enthalpies of fusion and crystallization of polymers by differential scanning calorimetry (2015).

[17] TA Orchestrator User Manual (v7.2.0.4). TA Instruments – Waters LLC, New Castle (2008).

[18] Galuppi L., Royer-Carfagni G.F., Effective thickness of laminated glass beams: new expression via a variational approach. Engineering Structures; 44, 53-67 (2012).

[19] López-Aenlle M. and Pelayo F. Dynamic effective thickness in laminated-glass beams and plates. Composites Part B Engineering, 67, 332–347 (2014).

[20] Tzikang, C., Determining a prony series for a viscoelastic material from time varying strain data. NASA Langley Technical Report Server (2000).

[21] Emri, I., Von Bernstorff, B.S., Cvelbar, R., Nikonov, A., Re-examination of the approximate methods for interconversion between frequency-and time-dependent material functions. Journal of non-Newtonian fluid mechanics, 129, 75-84 (2005).

[22] Park, S.W., Schapery, R.A., 1999. Methods of interconversion between linear viscoelastic material functions. Part I—a numerical method based on Prony series. International journal of solids and structures. 36, 1653-1675 (1999). doi:10.1016/S0020-7683(98)00055-9.

[23] Abaqus User's Manual, Dassault Systémes Simulia Corp., Providence, Rhode Island, USA (2012)

[24] Fröling M., Persson K., Computational methods for laminated glass. Journal of engineering mechanics, 10.1061/(ASCE)EM.1943-7889.0000527, 780-790 (2013).

[25] Brincker, R., Ventura, C., Introduction to operational modal analysis. Wiley (2015).

[26] Ewins D.J., Modal testing: theory, practice and application (2nd Ed.). John Wiley & Sons Ltd. Hertford (2000).

[27] Maia M.M., Silva M.M. et al. Theoretical and experimental modal analysis. Research Studies Press and John Wiley & Sons Ltd., Hertford (2007).

[28] Jones D.I.G., Handbook of viscoelastic vibration damping. John Wiley & Sons, Ltd., New York (2001).

[29] Gersch W., On the Achievable accuracy of structural system parameter estimates. Journal of sound and vibration, 34(1), 63-79 (1974).

Figure Captions:

Figure 1. General steps of the time-temperature superposition method.

Figure 2: Schematic of the master curve creation process

Figure 3. Example of relaxation modulus master curves at different temperatures.

Figure 4: Relaxation curves at different temperatures for the PVB.

Figure 5: Storage modulus curves at different temperatures for the PVB.

Figure 6: Temperature sweep at 1 Hz from -25^oC to 65^oC for the PVB.

Figure 7: Overlay curve of PVB (left) and experimental a_T^{exp} (right) for a reference temperature of 20^oC

Figure 8. Comparison of the WLF model when T_s, T_g or a temperature within the range $T_g < T < T_s$ are used (left) and final master curve of the PVB for $T_s = 50^oC$ (right).

Figure 9. Overlay complex modulus curve for the PVB at 35^oC.

Figure 10. Generalized Maxwell model.

Figure 11. Complex modulus of the PVB obtained by interconversion from the relaxation Prony coefficients at 20^oC.

Figure 12. Finite element models for the laminated glass plate and beam.

Figure 13. Displacement of central point of the laminated glass plate.